



Investigation of Anomalous Behavior in Metallic-Based Materials Under Compressive Loading

Christopher M. Gil and Cliff J. Lissenden
Pennsylvania State University, University Park, Pennsylvania

Bradley A. Lerch
Lewis Research Center, Cleveland, Ohio

The NASA STI Program Office . . . in Profile

Since its founding, NASA has been dedicated to the advancement of aeronautics and space science. The NASA Scientific and Technical Information (STI) Program Office plays a key part in helping NASA maintain this important role.

The NASA STI Program Office is operated by Langley Research Center, the Lead Center for NASA's scientific and technical information. The NASA STI Program Office provides access to the NASA STI Database, the largest collection of aeronautical and space science STI in the world. The Program Office is also NASA's institutional mechanism for disseminating the results of its research and development activities. These results are published by NASA in the NASA STI Report Series, which includes the following report types:

- **TECHNICAL PUBLICATION.** Reports of completed research or a major significant phase of research that present the results of NASA programs and include extensive data or theoretical analysis. Includes compilations of significant scientific and technical data and information deemed to be of continuing reference value. NASA's counterpart of peer-reviewed formal professional papers but has less stringent limitations on manuscript length and extent of graphic presentations.
- **TECHNICAL MEMORANDUM.** Scientific and technical findings that are preliminary or of specialized interest, e.g., quick release reports, working papers, and bibliographies that contain minimal annotation. Does not contain extensive analysis.
- **CONTRACTOR REPORT.** Scientific and technical findings by NASA-sponsored contractors and grantees.

- **CONFERENCE PUBLICATION.** Collected papers from scientific and technical conferences, symposia, seminars, or other meetings sponsored or cosponsored by NASA.
- **SPECIAL PUBLICATION.** Scientific, technical, or historical information from NASA programs, projects, and missions, often concerned with subjects having substantial public interest.
- **TECHNICAL TRANSLATION.** English-language translations of foreign scientific and technical material pertinent to NASA's mission.

Specialized services that complement the STI Program Office's diverse offerings include creating custom thesauri, building customized data bases, organizing and publishing research results . . . even providing videos.

For more information about the NASA STI Program Office, see the following:

- Access the NASA STI Program Home Page at <http://www.sti.nasa.gov>
- E-mail your question via the Internet to help@sti.nasa.gov
- Fax your question to the NASA Access Help Desk at (301) 621-0134
- Telephone the NASA Access Help Desk at (301) 621-0390
- Write to:
NASA Access Help Desk
NASA Center for Aerospace Information
7121 Standard Drive
Hanover, MD 21076



Investigation of Anomalous Behavior in Metallic-Based Materials Under Compressive Loading

Christopher M. Gil and Cliff J. Lissenden
Pennsylvania State University, University Park, Pennsylvania

Bradley A. Lerch
Lewis Research Center, Cleveland, Ohio

National Aeronautics and
Space Administration

Lewis Research Center

Trade names or manufacturers' names are used in this report for identification only. This usage does not constitute an official endorsement, either expressed or implied, by the National Aeronautics and Space Administration.

Available from

NASA Center for Aerospace Information
7121 Standard Drive
Hanover, MD 21076
Price Code: A03

National Technical Information Service
5287 Port Royal Road
Springfield, VA 22100
Price Code: A03

INVESTIGATION OF ANOMALOUS BEHAVIOR IN METALLIC-BASED MATERIALS UNDER COMPRESSIVE LOADING

Christopher M. Gil and Cliff J. Lissenden
Pennsylvania State University
University Park, Pennsylvania 16802

Bradley A. Lerch
National Aeronautics and Space Administration
Lewis Research Center
Cleveland, Ohio 44135

SUMMARY

An anomalous material response has been observed under the action of applied compressive loads in fibrous SiC/Ti (both Ti-6242 and Ti-15-3 alloys) and the monolithic nickel-base alloy IN-718 in the aged condition. The observed behavior is an increase, rather than a decrease, in the instantaneous Young's modulus with increasing load. This increase is small, but can be significant in yield surface determination tests, where an equivalent offset strain on the order of $10\ \mu\epsilon$ (10×10^{-6} m/m) is being used. Stiffening has been quantified by calculating offset strains from the linear elastic loading line. The offset strains associated with stiffening during compressive loading are positive and of the same order as the target offset strains in yield surface determination tests. At this time we do not have a reasonable explanation for this response nor can we identify a deformation mechanism that might cause it. On the other hand, we are not convinced that it is an artifact of the experimental procedure because a number of issues have been identified and seemingly ruled out. In fact, stiffening appears to be temperature dependent, since it decreases as the temperature increases.

INTRODUCTION

The experimental work described in this report is part of an ongoing effort between Pennsylvania State University and NASA Lewis Research Center to map out flow surfaces for silicon carbide/titanium in multi-dimensional stress space. These flow surface experiments involve loading a specimen multiaxially until plastic behavior begins to occur and then unloading before significant plastic flow occurs. This is done several times on the same specimen using different ratios of stress components until a surface is mapped out in stress space.

The definition of plastic flow that is used in these experiments is critical. Several definitions of yielding, commonly used to indicate the onset of plastic flow, and associated experimental techniques are reviewed by Khan and Wang (1993) and Hecker (1976). One can expect different results depending on the definition that is chosen. The definition of yielding chosen by the authors for this study involves detecting offset strains 'on the fly,' that is, offsets from the linear elastic loading line are determined under load, not after unloading. This method greatly expedites experimental detection of yielding, but relies on the assumption that the offset strains are directly related to permanent set. We expect a one-to-one relationship between the maximum offset strain and the permanent set if the initial loading and unloading moduli are equal and loading and unloading rates are equal. By seeking a very small offset, on the order of 10×10^{-6} m/m (or $10\ \mu\epsilon$), the change in internal state is minimized and multiple loading excursions (probes) can be conducted on the same specimen to map out the yield surface. This definition of yielding is very similar to the proportional limit definition. Further, it removes any concerns about specimen to specimen scatter in the yield surface since the same specimen is used for each probe. In addition, this method is cost effective in terms of the number of specimens required.

Similar multiprobe single-specimen yield surface experiments have been successfully conducted by a number of researchers on solution annealed monolithic materials (e.g., Phillips et al., 1972; Liu and Greenstreet, 1976; Helling et al., 1986; Wu and Yeh, 1991) as well as on an annealed boron-aluminum composite (Dvorak et al., 1988; Nigam et al., 1994a,b). Furthermore, the experimental setup used in the current study was implemented by Lissenden et al. (1997) to determine flow surfaces for solution annealed type 316 stainless steel at elevated temperature. Attempts to experimentally determine flow surfaces on a unidirectional SiC/Ti composite tube have been unsuccessful to date because of an anomalous response,

termed stiffening, under compressive loading. Stiffening is characterized by an increase in the modulus during loading, which creates an offset from the initial loading curve that is often comparable in magnitude (but opposite in sign) to the target value of the strain offset that is sought (fig. 1). The stiffening response appears to be more or less nonlinear elastic and can result in the false detection of yielding in the experiments described above.

The observation of stiffening led to a re-evaluation of the strain measurement apparatus and experimental procedure. After a thorough investigation, all of the equipment was determined to be functioning properly and giving reproducible results. However, the anomalous behavior persisted. This was perplexing since identical tests on solutioned 316 stainless steel were conducted successfully, yet the anomalous behavior prevented the tests on the composite tubes from being successful. In the process of validating the experimental setup and procedures, tubular Inconel 718 (IN-718) specimens were tested. It was found that thermally aged IN-718 exhibited stiffening, while solution annealed IN-718 did not.

To further study stiffening under pure axial loading, thick SiC/Ti-15-3 plates were cut into dogbone specimens. Several unidirectional SiC/Ti-15-3 specimens were available, although the titanium matrix was a different alloy than that in the SiC/Ti-6242 tubular specimens. Various loading rates and sequences were employed over a wide range of temperatures (23 to 649 °C). Unfortunately, these tests were complicated by the presence of bending. The aim of this report is to document the factors that were examined and present our current understanding of the anomalous behavior observed in the various specimens. The next section details the experimental equipment and procedures as well as the specimens used in this study. Subsequently, the results are presented, with the room temperature results (where rate effects are expected to be minimal) separated from those obtained at elevated temperature. Finally, the findings are summarized.

EXPERIMENTAL PROCEDURE

Our ongoing research program entails experimental determination of flow surfaces using axial-torsional loading. Toward this end, axial and torsional tests have been conducted on type 316 stainless steel (Lissenden et al., 1997), Inconel 718, and SiC/Ti-6242 tubular specimens, each having different dimensions. Additionally, axial tests were conducted on SiC/Ti-15-3 specimens having a rectangular cross section. In the remainder of this report we will refer to these as either tubular or thick plate specimens. We note that this experimental procedure requires that we assume the initial material response to be linear elastic.

Test Equipment

Experiments were conducted on one of two biaxial servohydraulic MTS machines having an axial load capacity of $\pm 222\,500$ N (50 000 lb) and a torque capacity of ± 2260 N-m (20 000 in.-lb). Water-cooled, hydraulically actuated grips were used to grip the specimens. The top grip remained fixed throughout the test. The bottom grip is attached to an actuator capable of independent rotation and axial translation. Rotational and translational movements of the actuator are independently controlled by an MTS 448 electronic controller on the machine used for testing thick plate specimens and an MTS 458 electronic controller on the machine used for testing tubular specimens. Both the 448 and the 458 allow for rotational control by angle, torque, or shear strain and translational control by displacement, load, or axial strain.

All tests were controlled by a 486 personal computer using custom written FORTRAN software. Digital-to-analog (D/A) and analog-to-digital (A/D) converters were used to command the controllers and for electronic data collection, respectively. In addition, X-Y chart recorders were used to monitor the output signals while the tests were being performed.

Axial and shear strains were measured by an extensometer and in some cases strain gages were also used. The extensometer is a standard off-the-shelf, water-cooled MTS biaxial model (fig. 2) with a gage length of 25 mm. Micro-measurements precision strain gages (Type EA-06-125BZ-350) having an electrical resistance of 350 Ω and a gage length of 3.2 mm were installed on one or both sides of select thick plate specimens that were to be tested at room temperature. A strain gage conditioner capable of handling multiple strain gages was used, employing an excitation voltage of 4 V and a calibration factor of 1000 $\mu\epsilon/V$.

A 5-kW Ameritherm induction heating system with three adjustable coils, described by Ellis and Bartolotta (1997), was used to heat the thick plate specimens, then hold the temperature constant, in elevated temperature tests. Three type K thermocouples were spot welded to the gage section of the specimen, with the center thermocouple used to control the temperature. The two remaining thermocouples were used to ensure a thermal gradient in the gage section of within ± 1 percent of the desired testing temperature.

Specimens

SiC/Ti.—A total of seven [0]₃₂ SiC/Ti-15-3 thick plate specimens were tested in tension and compression. Each specimen contained 35 percent by volume SCS-6 silicon carbide fibers aligned longitudinally to reinforce a Ti-15-3 matrix. The specimens were processed by consolidating layers of Ti-15-3 foil and SiC fibers to achieve a total thickness of approximately 7.6 mm. This thickness was sufficient to obviate buckling under the applied compressive loads. The specimens were then aged at 700 °C for 24 hr in a vacuum. Each specimen was 203.2 mm long and had the geometry shown in figure 3(a). At each end, 51 mm long by 12.7 mm wide by 2.4 mm thick stainless steel tabs were bonded to either side of the specimen to fill the collet gap in the grips and ensure that the proper gripping pressure was applied. Approximately 44.5 mm of each end of the specimen was gripped. The gripping force was obtained by applying a hydraulic pressure of 30 to 35 MPa to the grips, depending on the expected maximum load for the test. The grip pressure was chosen sufficiently high to prevent slippage and yet low enough to minimize damage to the specimen ends. Splitting of composite specimen ends is known to occur if the grip pressure is too high. Five of the seven specimens were in the virgin state at the beginning of this study. The other two specimens had been lightly loaded in a previous program.

One tubular SiC/Ti-6242 specimen was used in this study. The SCS-6 fibers are oriented along the axis of the tube, which was fabricated using the foil-fiber-foil technique. The fiber volume fraction has not yet been measured, but is nominally 0.25. The tube has inner and outer diameters of 20.7 and 23.3 mm, respectively, and was cut to a length of 203 mm. It was gripped by a fixture that was designed to transfer stress as uniformly as practical without crushing or splitting the tube.

Monolithic.—The type 316 stainless steel tubular specimen, described in detail by Lissenden et al. (1997), is 229 mm long, and has a dogbone shape. The gage section has inner and outer diameters of 22 and 26 mm, respectively. The Inconel 718 tubular specimens are shown in figure 3(b), are 229 mm long, have a dogbone shape, and the gage section inner and outer diameters are 15.9 and 21 mm, respectively.

Room Temperature Tests

Thick plate specimens.—Each test was run in axial load and rotation control with the rotation remaining fixed throughout the test (i.e., a uniaxial test). The axial load (engineering stress) was increased monotonically and the initial Young's modulus, E , was determined by linear regression during a predefined stress range. A constant data sampling interval was used throughout the test. The stress range was determined by past experience and represented a balance between gathering enough data to accurately calculate the modulus and yet not exceeding the proportional limit. Once the modulus was determined, the strain offset from the linear elastic loading line, ϵ^{off} , was calculated from the total strain, ϵ , the applied stress, σ , the prestress, σ_0 , and the modulus,

$$\epsilon^{off} = \epsilon - \frac{\sigma - \sigma_0}{E}$$

and continually compared to a target value (usually 10 $\mu\epsilon$). When the offset strain reached the target value, the specimen was unloaded at a rate four times that of the loading rate. The increased unloading rate was used to expedite the tests since several repeats of each test were commonly performed.

Three loading sequences were used in the experiments, they are

- (1) A single cycle of tension followed by a single cycle of compression
- (2) A single cycle of compression followed by a single cycle of tension
- (3) Consecutive compression cycles

Loading rates of 1.69, 6.89, and 34.5 MPa/sec were used at 482 °C. Limited data showed that the average Young's modulus for compressive loading increased by about 1.4 percent because of the increased loading rate at this temperature. No similar data were gathered at room temperature.

Tubular specimens.—Proportional axial-torsional loads were applied to the type 316 stainless steel tube and the SiC/Ti-6242 tube and the procedure is described in detail by Lissenden et al. (1997). For this work the nature of the biaxial loading is unimportant and will not be discussed further. Regarding the Inconel 718 tubular specimens, we will present results for compressive axial loading only.

Elevated Temperature Tests

Results from elevated temperature tests are reported only for the thick plate specimens. In general, the same procedure that was used at room temperature was also used at elevated temperature. All tests on thick plate specimens were performed using loading sequence 1 (above) at 427, 482, 538, and 649 °C. At these temperatures it is difficult to measure strain with strain gages, therefore only the extensometer was used. The electronic noise in the strain signal, caused by the induction heating system, was checked prior to testing and was determined to be within acceptable limits based on results from a prior study (Lissenden et al., 1997).

RESULTS

Experimental results for different materials will be presented in chronological order; that is,

- (1) Type 316 stainless steel tubular specimens, where the material response was as expected
- (2) SiC/Ti-6242 tubular specimens, where anomalous material response was first detected
- (3) SiC/Ti-15-3 thick plate specimens, where the anomalous response was studied in detail, and which represent the bulk of the results presented in this report
- (4) IN-718 tubular specimens in the solution annealed and thermally aged states

Type 316 Stainless Steel

Results from yield surface experiments on solution annealed 316 stainless steel are presented by Lissenden et al. (1997). Here we will only look at the axial stress-strain response from one typical probe of a yield surface at room temperature. Strains were measured during proportional loading probing experiments on specimen 316SS18 with the extensometer and strain gages. The axial stress-strain response from probe number 1 (a 12° probe angle, predominantly axial tension) of surface determination run number 6 is shown in figure 4(a); shear stresses ($\sigma_{12} = 0.2126\sigma_{11}$) and strains were also present but are not shown here. Only the strains measured by the extensometer are shown for clarity, but the strains measured by the strain gages are quite similar. The initial response is linear elastic with the linearly regressed stress-strain equations in the strain range $0 < \epsilon < 150 \mu\epsilon$ being

$$\sigma = 196\,510\epsilon + 0.11652 \text{ (Extensometer)}$$

$$\sigma = 190\,970\epsilon + 0.13285 \text{ (Strain gages)}$$

with σ in MPa and ϵ in m/m.

These equations represent the elastic loading lines for the extensometer and strain gages, respectively. Figure 4(b) shows the (axial) offset strain as a function of (axial) total strain for both the extensometer and strain gages. Neglecting the rather wide scatter band in the data, the offset strain starts to increase at a total strain of $\sim 400 \mu\epsilon$ and once the load is removed the offset strain remains as permanent set. This is typical of plastic deformation in metals and strongly suggests that the offset strain is an excellent indicator of the permanent set. Notice that, while the equations of the elastic loading lines were different for the extensometer and the strain gages (that is, a 2.8 percent difference in Young's modulus), the offset strains measured were nearly identical.

SiC/Ti-6242 Tubular Specimens

In an effort to study the multiaxial inelastic response of SiC/Ti, we attempted to conduct yield surface tests on SiC/Ti-6242 tubular specimens. Figure 5 shows the axial stress-strain response and the axial offset strain as a function of the total axial strain for a probe angle of -168° (predominantly axial compression, $\sigma_{12} = -0.2126\sigma_{11}$). Again, shear stresses and strains were present, but are not shown. Since we had anticipated the center of the flow surface to be shifted in the compressive stress direction because of residual stresses, we started each probe at a compressive stress of approximately 420 MPa. The elastic loading line in the strain range $-2500 < \epsilon < -2200 \mu\epsilon$ is

$$\sigma = 189\,612\varepsilon + 1.2907$$

and although the stress-strain response appears to be linear throughout, small offset strains are present. Strangely enough, these offset strains have positive, rather than negative, magnitudes and therefore describe stiffening. Additionally, the offset strain decreased during unloading more than it had increased during loading, resulting in a very small ($\sim 3\mu\varepsilon$) compressive permanent set. While the stiffening observed during loading is very representative of what we observed for compressive loading, and occasionally torsional loading, the calculated offset strains during unloading were somewhat erratic.

Even though these offset strains are small, they are statistically meaningful. We have determined the 95 percent confidence limits on the linearly regressed loading line and extrapolated them up to the maximum load. Doing so we found that the measured stress-strain response falls above the upper limit. Since there were 250 data points used in the regression and the correlation factor was 0.99958, and also because this strain range was very successful for determining the elastic loading line during tensile loading, we are confident that our procedure is valid.

SiC/Ti-15-3 Thick Plate Specimens

We wanted to closely examine the tensile and compressive behavior of SiC/Ti, but rather than working with the few available tubular specimens, we used thick plate specimens that originated from a different program. These plate specimens have the same SCS-6 fiber and consequently the same weak interface as the tubular specimens. Therefore, the behavior of the thick plates should be similar to the tubes. Unfortunately, these plates were not entirely flat, which complicates the interpretation of the results.

Room Temperature

Loading sequence 1 tests, that is tension followed by compression, were conducted at room temperature using an applied stress rate of 1.67 MPa/sec. The coefficients of the elastic loading line,

$$\sigma = E\varepsilon + \sigma_0$$

where E is Young's modulus and σ_0 is a prestress, are shown in table I for four different tests. Each test was started with the stress and strain readings as close to zero as practical. There is a 1 percent variation in the tensile Young's modulus and a 0.2 percent variation in the compressive Young's modulus. The compressive Young's modulus is approximately 1 percent larger than the tensile Young's modulus in these four tests. The larger (negative) prestresses for compressive loading are an indication of the permanent set that occurred because of the tensile loading.

The stress-strain response as well as the calculated offset strain as a function of the total strain for tensile loading are shown in figure 6. Unloading was triggered by the calculated offset strain attaining a target value of $\pm 10\mu\varepsilon$ in this and all subsequent tests, unless otherwise noted. Additionally, strains were measured by the extensometer unless reported to the contrary. The maximum stress for the tensile loading shown in figure 6(a) was 450 MPa. Figure 6(b) shows that the offset strains were essentially zero during elastic loading (until the total strain was approximately 1000 $\mu\varepsilon$) and are positive thereafter, suggesting plastic deformation. The permanent set turned out to be more than twice the maximum offset during loading. This difference could be due to measurement problems with the extensometer upon reversal of load or possibly rate-dependence of Young's modulus (a viscoelastic effect).

For experimental expediency, unloading was done at four times the loading rate. We have no data indicating that Young's modulus is loading rate-dependent at room temperature, but as mentioned previously, it does appear to be slightly rate-dependent at elevated temperature. If the increased unloading rate were to increase the Young's modulus by a very modest 0.5 percent, then the offset strain at zero load after elastic unloading would be 22 $\mu\varepsilon$. Additional experiments are required to determine if this is the cause of the large apparent permanent set, or if it is due to load reversal effects on the mechanical extensometer. It could be that the load reversal re-seats the extensometer rods in their indents. This is not normally a problem, but these tests demand extremely high resolution measurement of strain.

The strain response exhibited stiffening (fig. 7) for compressive loading, which prompted unloading when a +10 $\mu\varepsilon$ offset strain was obtained at a stress of -600 MPa. During unloading the offset strain decreased below zero, resulting in a permanent set after unloading of approximately $-20\mu\varepsilon$ (fig. 7(b)) and suggesting

that plastic deformation occurred even though the material exhibited stiffening. Several other tension and compression cycles were performed on various specimens with similar results.

The loading rate appeared to have no effect on whether stiffening was observed. Stiffening was observed for loading rates of 1.67 and 6.89 MPa/sec. However, the maximum stresses for these two rates were quite different, -758 MPa for the slower rate and -414 MPa for the faster rate. When stiffening occurred, the target value was attained for a wide range of stresses, even for the same loading rate.

Loading sequence 2 tests, that is compression followed by tension, were conducted next, to determine if the tensile load reversal and possibly some associated internal stresses were responsible for stiffening. A virgin specimen was tested and no stiffening was observed in the extensometer data. It was re-tested using loading sequence 1 and, again, no stiffening was observed. Therefore a non-virgin specimen, PL-6-5, which had exhibited stiffening in the loading sequence 1 tests, was tested and no stiffening in either compression or tension was observed in the extensometer data (compression shown in fig. 8(a)). This test was repeated on the same specimen after being removed and then reinstalled in the grips. The results are shown in figure 8(b), where stiffening is indicated. These are contradictory results, that, as it turns out, can be explained by the actual strain distribution, which is not known in this case because only the extensometer was used. However, the load sequence can be ruled out as the cause of stiffening because some of the results for loading sequence 2 tests did show stiffening.

To investigate the repeatability of stiffening, compressive cycling to a fixed stress level rather than to a target offset strain was performed (loading sequence 3). A nonvirgin specimen (PL-6-5) was loaded to approximately -500 MPa (a higher magnitude of stress than previous tensile cycles) multiple times in an attempt to remove any internal stresses created by previous tensile loading. No tensile loading was applied during this series of experiments. This loading could also provide guidance as to whether stiffening is associated with plastic strain, since loading (from zero stress) multiple times to a fixed stress level produces minimal, if any, plastic deformation after the first cycle. Stiffening was observed with each loading and the magnitude of the offsets appeared to be random as shown in figure 9. There is no apparent relationship between the magnitude of the stiffening offset and the cycle number, indicating that stiffening is not directly related to plastic deformation. Further, to a close approximation, the stiffening response is nonlinear elastic with the offsets at zero stress from each of the five tests being in the range of 2 to 5 $\mu\epsilon$.

Is there another mechanism that could be responsible for the absence of stiffening observed for the virgin specimen discussed above? Let us consider bending. The specimens are initially warped, additionally the test machine's load train is not perfectly aligned and we are applying compressive loads. Therefore, some bending is anticipated. To quantify it, we measured strains with strain gages bonded to opposite sides of the specimen. In one series of tests the offset strains are determined to be as shown in figures 10(a) to (c) for consecutive loadings to maximum compressive stresses of 1034, 690, and 690 MPa, respectively; in another series they are as shown in figures 10(d) to (f) for consecutive loadings to maximum compressive stresses of 552, 690, and 690 MPa, respectively. Each of the three tests shown in figures 10(a) to (c) are from the same experimental setup. That is, the specimen was installed in the grips and three loading cycles (sequence 1) were applied. The same is true for the results shown in figures 10(d) to (f). We believe stiffening to be a different phenomenon than bending because in these tests strain gages on both sides of the specimen indicated stiffening. The justification is provided below.

There are two primary factors contributing to bending in these tests: (1) the initial warpage of the specimen, and (2) misalignment of the load train in terms of the axis of the top grip not being collinear with the axis of the bottom grip because of either an offset or a misalignment angle, or both. It is not uncommon for metal matrix composites to be warped since large residual stresses can develop during the cool-down stage of processing because of the thermal coefficient of expansion (CTE) mismatch between the fibers and the matrix (e.g., Bigelow, 1993). Furthermore, misaligned fibers can lead to a nonuniform strain distribution during cool down and also cause warping of the specimens. Warping of one specimen was measured by placing it on a surface plate and taking measurements using a dial gage along the length of the specimen. This specimen was found to be bent about one side and slightly twisted about the fiber axis (see table II).

An analysis of the grip alignment on the test machine showed that the grips were misaligned, front to back, such that the front surface of a nonwarped specimen would experience a compressive strain of -48 $\mu\epsilon$ and a tensile strain of equal magnitude on the opposite side when gripped. One strain gage was mounted on each side of a SiC/Ti-15-3 specimen, and tests were conducted in which the specimen was loaded in tension and compression. The specimen was taken out of the grips and rotated 180° about the loading axis, then loaded again in tension and compression. This process was repeated several times. Each time, upon gripping the specimen, the output of the strain gages was recorded to quantify bending prior to loading. It was discovered that when gripped, the specimen was being bent in the opposite direction than it was initially warped, as if being straightened. This also suggested that the warpage of the specimen was larger and more influential than the machine misalignment.

When the specimen was oriented such that the specimen warpage and the test machine misalignment coincided to induce maximum bending, a large amount of stiffening was present on the side of the specimen that was originally convex (strain gage 1 and extensometer, see fig. 11). On the opposite side, stiffening could be masked by the additional compressive strains caused by bending (strain gage 2, see fig. 11). When the specimen was oriented in the opposite direction, such that the initial warpage of the specimen was counter to the bending caused by the misalignment of the test machine, there was stiffening observed on both sides of the specimen, suggesting that the bending taking place was not significant.

Bending strains varied from setup to setup depending on the amount of specimen warpage and how the specimen was gripped. The application of the tabs may also have an effect on bending. Furthermore, stiffening may or may not be evident when measuring strains on only one side of a specimen, depending on the relative magnitudes of stiffening and bending. One specimen, tested in compression, displayed a large positive offset strain on one side and a negative offset strain (suggesting plasticity) on the other side (fig. 11). This could explain why the specimen shown in figure 8(a) displayed no apparent stiffening on the side of the specimen where the strain was measured.

Up to this point all offset strains have been calculated by neglecting the bending stresses. In order to include the bending stresses we need to know the location of the neutral axis. A photomicrograph of the cross section of a specimen shows that there are 32 rows of fibers and that each row has about 50 fibers. Suppose that instead of all rows having 50 fibers in them, that the sixteen rows on one half only have 49 fibers. This places the neutral axis at $0.5025t$, where t is the thickness of the specimen. This is probably a much worse case than reality, and yet there is very little change in the location of the neutral axis. Our strain gage data acquired during gripping the specimen contains significant scatter, but places the neutral axis between $0.496t$ and $0.558t$, assuming a linear strain field. Therefore, we do not have sufficient data to suggest anything other than that the neutral axis is in the center of the plate.

Strain gage data from each side of the specimen were averaged to obtain an estimate of the effective material behavior independent of bending (fig. 11). This effective behavior shows a large reduction of the stiffening when the bending is averaged out. In the complete absence of bending, stiffening may be observed on both sides of the specimen. When no bending is present, one would expect the stiffening offset to reverse at some point prior to failure.

In the above discussion, bending about the other axis, that is the width of the specimen, has been thought to be small and therefore was neglected. Future experiments are planned that will demonstrate without any doubt whether or not stiffening is a mechanism separate from bending.

Having exhausted several types of loading sequences in an attempt to achieve repeatable results absent of stiffening, a specimen was loaded in compression beyond the $+10 \mu\epsilon$ stiffening offset in order to determine when, or if, the offset would reverse direction and the material would yield and begin to flow plastically. The specimen was loaded to a compressive stress in excess of -1600 MPa with no indication of a reversal in the offset strain. The offset strain exceeded $+600 \mu\epsilon$, at which time the load was manually removed. We suspect that bending becomes more severe with increased compressive load, but strain was only measured on one side of the specimen. Based on results from Newaz, et al. (1996) who tested a similar SiC/Ti-15-3 composite in compression, it is possible that the -1600 MPa was not high enough to cause yielding in compression. Newaz found the proportional limit to be approximately -2200 MPa. However, it is unlikely that our specimens could have been subjected to the same magnitude of stress without the use of buckling guides.

Elevated Temperature

Thick plate specimens were also tested at 427, 482, 538, and 649 °C to determine the influence of temperature on measured response. Strains were measured only on one side of the specimen because it was not practical to mount an additional extensometer on the opposite side. Because of the uncertainty about the presence of bending, we are not able to make firm statements about whether any observed stiffening is related to material behavior or merely an artifact of bending.

In the first series of experiments, from which partial results are shown in figures 12 to 15, the loading rate was 1.67 MPa/sec and unloading (at four times the loading rate) was initiated when the absolute value of the offset strain reached $10 \mu\epsilon$. As expected, the maximum compressive stress present upon reaching the target value ($\pm 10 \mu\epsilon$) decreased as the temperature increased.

Temperature, °C	427	482	538	649
Maximum stress, MPa	517	310	172	103

The offset strains determined for compressive loading at 427 °C (fig. 12) were very similar to offset strains at room temperature that we called stiffening. Positive offset strains for compressive loading at 482 °C were minimal or absent altogether (fig. 13). At 538 and 649 °C, no significant positive offset strains occurred for compressive loading (figs. 14 and 15).

The unloading modulus appears to be higher than the loading modulus at 538 and 649 °C (figs. 14(a) and 15(a)). This could be because the unloading rate was four times faster than the loading rate. At temperatures of 427 °C, Castelli (Private communication from M.G. Castelli, 1997) has found Ti-15-3 to be slightly strain rate sensitive (i.e., the elastic modulus increases or decreases as the loading rate increases or decreases) and the strain rate sensitivity increases with further increases in temperature.

The material behavior at 427 °C was investigated further by conducting compression probes using a target value of $-10\ \mu\epsilon$, rather than its absolute value, to trigger unloading. Hence, a positive offset strain in excess of $10\ \mu\epsilon$ would not initiate unloading and a reversal in the offset strain rate followed by a reversal in the sign of the offset strain was possible. Figure 16 indicates that positive offset strains accumulated to approximately $+13\ \mu\epsilon$ before reversing and eventually reaching the target value of $-10\ \mu\epsilon$ at a compressive stress of $-932\ \text{MPa}$. In contrast to the positive offset strains shown in figure 12, the negative offset strains shown in figure 16 appear to be associated with permanent set. The reversal in offset strain at 427 °C is in contrast to the observed behavior at room temperature where no reversal was detected for the loads applied. Furthermore, the reversal in offset strain occurred at a relatively low stress.

The same test procedure was used at 482 °C, with the results from both tensile and compressive probes shown in figure 17 being typical of the tests performed at this temperature. There is a reasonably well-defined linear region followed by the initiation of offset strains that appear to be associated with permanent set. The target value was attained at a tensile stress of $157\ \text{MPa}$. Subsequently, the compressive stress was $241\ \text{MPa}$ when the target value was attained. The larger stress for compressive loading may reflect the existence of residual stresses from processing (of course, the residual stresses are expected to be much higher at room temperature).

Next, the effect of loading rate on achieving the target values of $+10\ \mu\epsilon$ for tension and $-10\ \mu\epsilon$ for compression was studied. Probes were conducted on a specimen at 482 °C using three different loading rates: 1.67, 6.89, and $34.5\ \text{MPa/sec}$. Overall, the tensile and compressive results shown in figure 18(a) for each test are reasonably symmetric with respect to the line $\sigma = -5\ \text{MPa}$; residual stresses could explain why the line of symmetry is not $\sigma = 0$. Notice that the loading rate was increased, then decreased, and finally increased again. In general, the maximum stress increased as the loading rate increased, which was expected because of the strain rate sensitivity. However, the results show that when the loading rate is changed, there is some dependence on the previous loading rate. In Test 7 (fig. 18(a)), the loading rate had been changed from 6.89 to $34.5\ \text{MPa/sec}$, and the stress level is smaller than in Tests 8 and 9. The reverse situation is true for Test 10, where the stress is larger during the first probe at $6.89\ \text{MPa/sec}$ than in Tests 11 and 12. This suggests that the underlying dislocation structure in the titanium matrix is affected by the previous cycle(s) and requires a few cycles to readjust itself to the new loading conditions. Additionally, there was commonly a positive offset strain that increased up to approximately $+30\ \mu\epsilon$ before reversing for compressive loading at a rate of $34.5\ \text{MPa/sec}$ (fig. 18(b)). This could be due to the specimen being more susceptible to bending as the compressive load becomes larger.

As mentioned previously, it was not practical to measure strain on both sides of the specimen at elevated temperature. However, most specimens were tested at room temperature first, where stiffening was observed in compression. The specimens were then heated to the desired test temperature without being removed from the grips. The room temperature results indicated that consistent behavior from a specimen is obtained as long as it remains gripped in the test machine. Therefore, since stiffening (now believed to be unrelated to bending) was observed at room temperature and the specimen was not removed from the grips prior to heating, we can infer that the reduction of stiffening behavior, or lack thereof, at elevated temperature is true behavior, and not a consequence of bending.

Finally, the effects of a larger, $20\ \mu\epsilon$, offset were investigated at 482 °C. Results from tension and compression probes conducted at a rate of $6.89\ \text{MPa/sec}$ using target values of 10 and $20\ \mu\epsilon$ are compared in figure 19. No stiffening is observed and there is little qualitative difference. However, we note that the effect of initial stiffening, when present, is expected to be less when a larger target value is used because the ratio of stiffening to target value is smaller. However, the question of whether the larger offset strain significantly changes the macroscopic material state must be investigated further.

Inconel 718

To determine whether stiffening is associated only with SiC/Ti composites; which are quite complex materials because they are heterogeneous, anisotropic, have residual stresses, and are susceptible to damage; or can occur in homogeneous monolithic materials, we also tested Inconel 718 (IN-718) at room temperature. Two material states were investigated, (1) solution annealed (1038 °C in argon for 1 hr, then air cooled) and (2) solution annealed (as previously described) and then thermally aged (720 °C in argon for 8 hr, cooled at 55 °C/hr to 620 °C, held for 8 hr, then air cooled). The loading cycle for each test consisted of four uniaxial probes to a target offset strain of $\pm 10 \mu\epsilon$: tension, compression, positive torque, and finally negative torque. Only results from the compression probes are shown and discussed because the results of the other three types of probes were routine. The loading rate was 1.38 MPa/sec and the unloading rate was four times faster.

Solution annealed.—The compressive stress-strain response for a solution annealed IN-718 tube is shown in figure 20(a) and the calculated offset strains are plotted as a function of the total strain for three consecutive tests in figure 20(b). Both the stress-strain response and the calculated offset strains indicate the presence of plastic deformation (i.e., that the offset strain correlates very well with the permanent set). The axial strain at which the target offset strain is attained increases slightly from Test 1 to Test 3 because of the small change in material state that occurs during each probe. This response agrees with our current understanding of the deformation of metallic materials.

Aged.—The compressive stress-strain response for a solution annealed then thermally aged IN-718 tube is shown in figure 21(a) and the calculated offset strains are plotted as a function of the total strain for three consecutive tests in figure 21(b). A statistical analysis was performed on the Test 3 data to verify that the calculated offsets were significant with respect to the linearly regressed elastic loading line. The 0.95 confidence limits were extrapolated to the point where the maximum stiffening offset strain occurred. Based on using 97 data points to regress the elastic loading line,

$$\sigma = 208\,261\epsilon - 1.973494$$

the 0.95 confidence limits on the elastic strain are $[-3966; -3960] \mu\epsilon$ at an applied compressive stress of 827 MPa, while the actual measured strain was $-3944 \mu\epsilon$. The 0.95 confidence limits are also shown in figure 21(b). Clearly, the positive offset strains are well outside these limits indicating that the stiffening is statistically significant.

CONCLUDING REMARKS

An anomalous material response has been observed under the action of applied compressive loads in fibrous SiC/Ti (both Ti-6242 and Ti-15-3 alloys) and the monolithic nickel-base alloy IN-718 in the aged condition. The observed behavior is an increase, rather than a decrease, in the instantaneous Young's modulus with increasing load. This increase is small, but can be significant in yield surface determination tests, where an equivalent offset strain on the order of $10 \mu\epsilon$ is being used. Stiffening has been quantified by calculating offset strains from the linear elastic loading line. The offset strains associated with stiffening during compressive loading are positive and of the same order as the target offset strains in yield surface determination tests. At this time we can offer no reasonable explanation for this response nor can we identify a deformation mechanism that might cause it. On the other hand, we are not convinced that it is an artifact of the experimental procedure because a number of issues have been identified and seemingly ruled out. They are

- The adequacy of the mechanical extensometer has been verified on IN-718 and type 316 stainless steel in the solution annealed condition. Its results are comparable to those obtained from strain gages.
- While bending was clearly present in some tests, its effects appeared to be minimal in others where stiffening was measured on both sides of a thick plate SiC/Ti-15-3 specimen. Thus, we believe bending and stiffening to be independent. We plan one more series of tests on IN-718 where strain gages will be bonded to each face of a square cross section to facilitate more complete quantification of bending effects.
- The offset strains associated with stiffening are statistically significant in that they fall outside of the 0.95 confidence limits for the extrapolated linear elastic loading line.

- Stiffening was observed in tests conducted on two completely separate test machines. The load cell and extensometer were calibrated and re-calibrated for this study. Additionally, the effect of grip pressure was studied to ensure that the specimen was not slipping.
- As the tests were conducted at higher and higher temperatures, the magnitude of stiffening decreased, suggesting that stiffening may be related to a temperature-dependent deformation mechanism.
- The majority of our data indicate that stiffening is essentially a linear elastic phenomenon.

REFERENCES

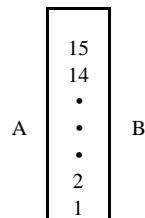
- Bigelow, C.A. (1993), Thermal Residual Stresses in a Silicon-Carbide/Titanium [0/90] Laminate. *J. Compos. Tech. Res.*, vol. 15, pp. 304–310.
- Dvorak, G.J., et al. (1988), An Experimental Study of Elastic-Plastic Behavior of a Fibrous Boron-Aluminum Composite. *J. Mech. Phys. Solids*, vol. 36, pp. 655–687.
- Ellis, J.R. and Bartolotta, P.A. (1997), Adjustable Work Coil Fixture Facilitating the Use of Induction Heating in Mechanical Testing. *Multiaxial Fatigue and Deformation Testing Techniques*, ASTM STP 1280, S. Kalluri and P.J. Bonacuse, Eds., ASTM, pp. 43–62.
- Hecker, S.S. (1976), Experimental Studies of Yield Phenomena in Biaxially Loaded Metals. *Constitutive Equations in Viscoplasticity: Computational and Engineering Aspects*, AMD vol. 20, ASME, New York, pp. 1–33.
- Helling, D.E., et al. (1986), An Experimental Investigation of the Yield Loci of 1100-0 Aluminum, 70:30 Brass, and an Overaged 2024 Aluminum Alloy After Various Prestrains. *J. Engng. Mater. Technol.*, vol. 108, pp. 313–320.
- Khan, A.S. and Wang, X. (1993), An Experimental Study on Subsequent Yield Surface After Finite Shear Prestraining. *Int. J. Plasticity*, vol. 9, pp. 889–905.
- Lissenden, C.J., et al. (1997), Experimental Determination of Yield and Flow Surfaces Under Axial-Torsional Loading. *Multiaxial Fatigue and Deformation Testing Techniques*, ASTM STP 1280, S. Kalluri and P.J. Bonacuse, Eds., ASTM, pp. 92–112.
- Liu, K.C. and Greenstreet, W.L. (1976), Experimental Studies to Examine Elastic-Plastic Behavior of Metal Alloys Used in Nuclear Structures. *Constitutive Equations in Viscoplasticity: Computational and Engineering Aspects*, AMD Vol. 20, ASME, New York, pp. 35–56.
- Newaz, G.M., et al. (1996), Inelastic Deformation Mechanisms in SCS-6/Ti-15-3 Metal Matrix Composite (MMC) Lamina Under Compression. *Life Prediction Methodology for Titanium Matrix Composites*, ASTM STP 1253, W.S. Johnson, J.M. Larsen, and B.N. Cox, Eds., ASTM, pp. 208–230.
- Nigam, H., et al. (1994a), An Experimental Investigation of Elastic-Plastic Behavior of a Fibrous Boron-Aluminum Composite: I. Matrix-Dominated Mode. *Int. J. Plasticity*, vol. 10, no. 1, pp. 23–48.
- Nigam, H., et al. (1994b), An Experimental Investigation of Elastic-Plastic Behavior of a Fibrous Boron-Aluminum Composite: II. Fiber-Dominated Mode. *Int. J. Plasticity*, vol. 10, no. 1, pp. 49–62.
- Phillips, et al. (1972), An Experimental Investigation of Yield Surfaces at Elevated Temperatures. *Acta Mechanica*, vol. 14, pp. 119–146.
- Wu, H.C. and Yeh, W.C. (1991), On the Experimental Determination of Yield Surfaces and Some Results of Annealed 304 Stainless Steel. *Int. J. Plasticity*, vol. 7, pp. 803–826.

TABLE I.—SiC/Ti ELASTIC LOADING LINE
COEFFICIENTS FOR TENSILE AND
COMPRESSIVE LOADING

Test	Tension		Compression	
	E, MPa	σ_0 , MPa	E, MPa	σ_0 , MPa
1	190 565	0.104337	191 351	-1.78900
2	189 369	0.047183	190 984	-3.85694
3	189 151	0.721945	191 216	-3.37030
4	189 092	0.439698	190 865	-4.08399

TABLE II.—FLATNESS MEASUREMENTS TAKEN AT
12.7 mm INTERVALS ALONG EACH SIDE OF SiC/Ti
THICK PLATE SPECIMEN

Position	A, μm	B, μm	Position	A, μm	B, μm
1	0	0	9	342.9	215.9
2	63.5	38.1	10	356.6	190.5
3	114.3	63.5	11	381.0	165.1
4	152.4	88.9	12	419.1	114.3
5	190.5	127.0	13	393.7	88.9
6	228.6	152.4	14	355.6	38.1
7	254.0	165.1	15	292.1	-63.5
8	292.1	190.5			



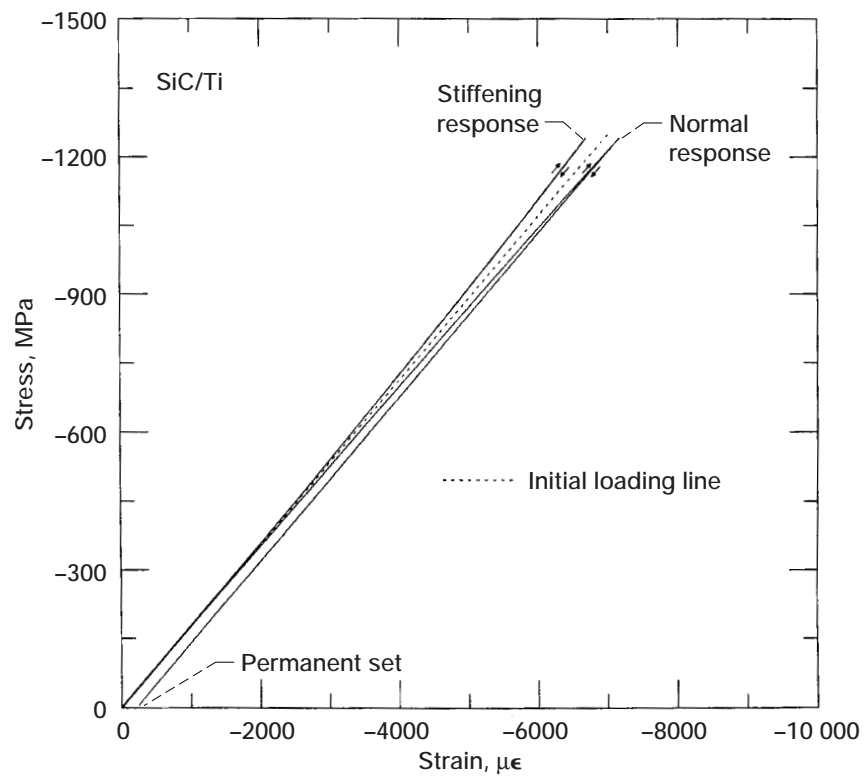


Figure 1.—Stiffening phenomenon in strain response for SiC/Ti composite.

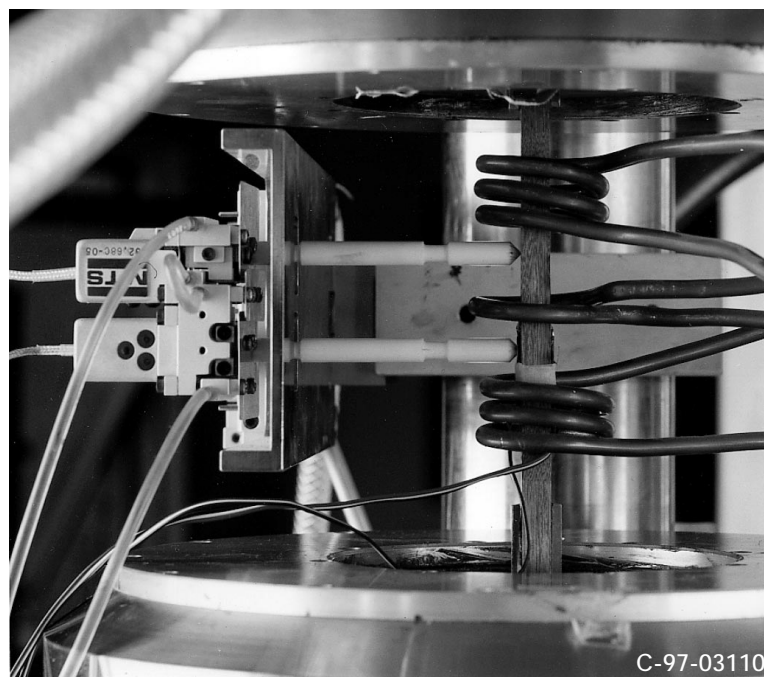


Figure 2.—Biaxial extensometer, induction heating coils, and SiC/Ti-15-3 thick plate specimen.

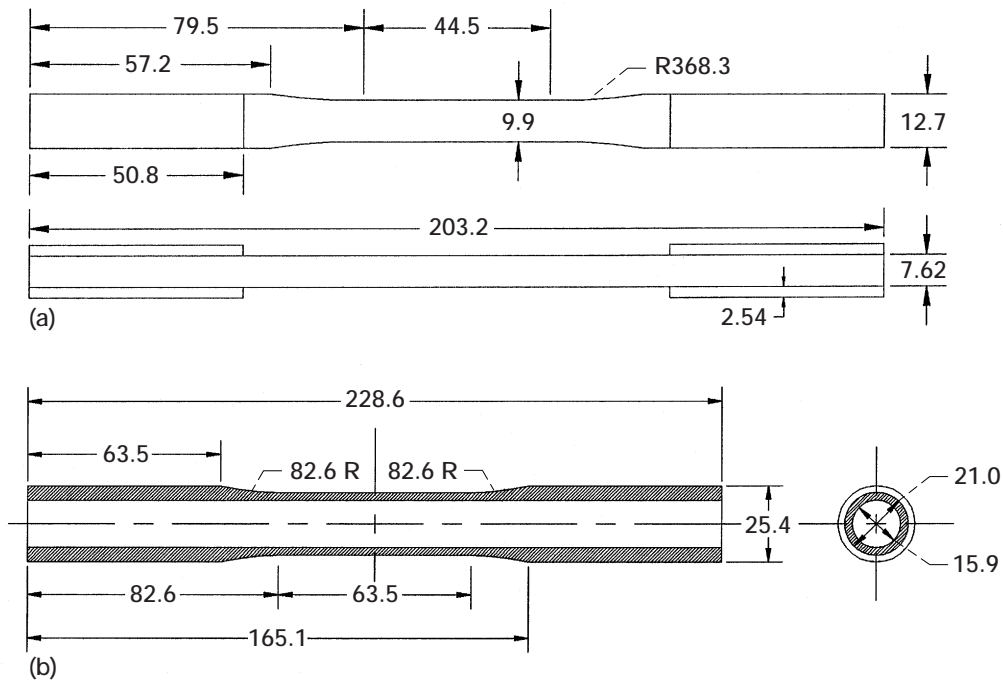


Figure 3.—Typical specimen geometries. (All dimensions in mm.) (a) SiC/Ti-15-3 thick plate. (b) Inconel 718 tube.

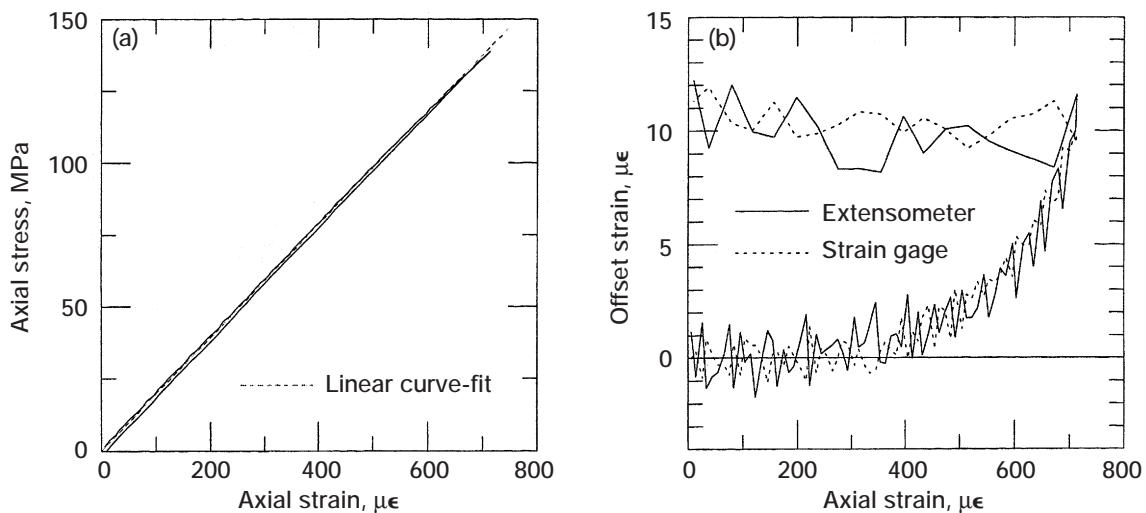


Figure 4.—Type 316 stainless steel response to yield surface probe at 12° in the axial-torque stress plane at 23 °C. (a) Axial stress-strain with linear loading line shown. (b) Axial offset strain-total strain indicating no stiffening.

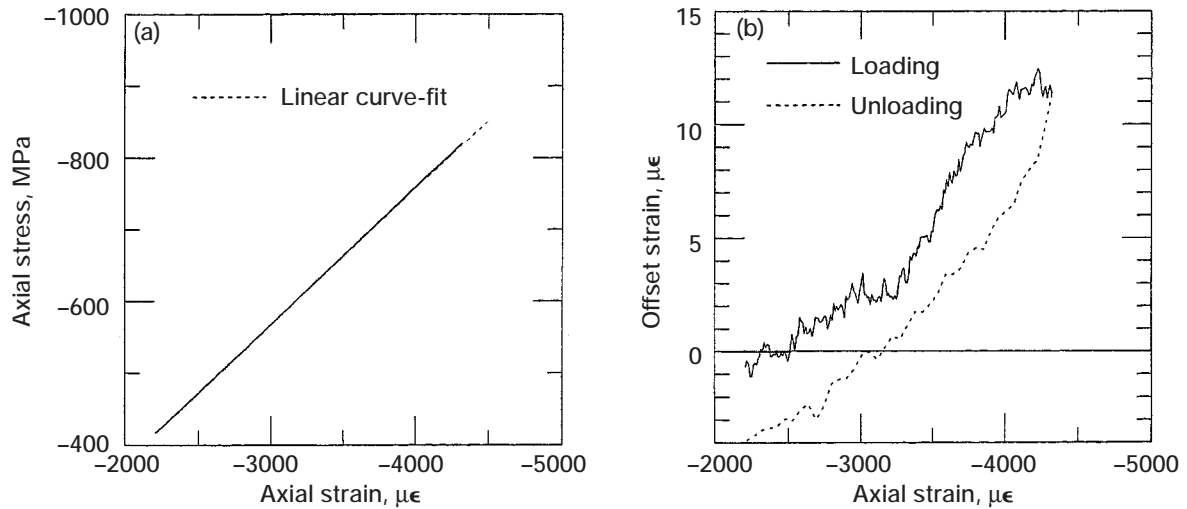


Figure 5.—SiC/Ti-6242 tube response to yield surface probe at -168° in the axial-torque stress plane at 23°C . (a) Axial stress-strain with linear loading line shown. (b) Axial offset strain-total strain indicating stiffening.

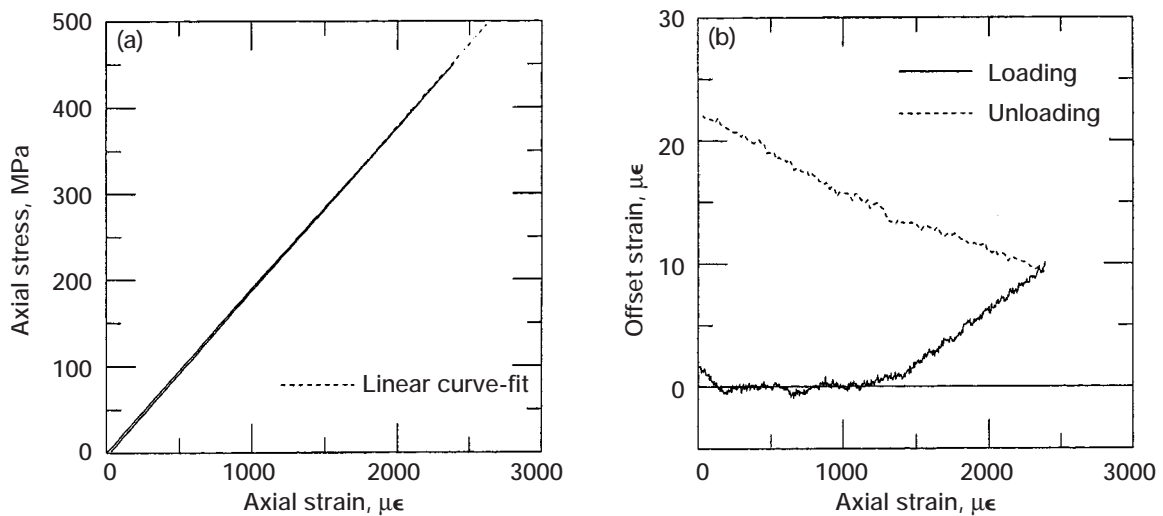


Figure 6.—SiC/Ti-15-3 thick plate response to tensile loading portion of loading sequence 1 at 23°C . (a) Stress-strain with linear loading line shown. (b) Offset strain-total strain indicating no stiffening.

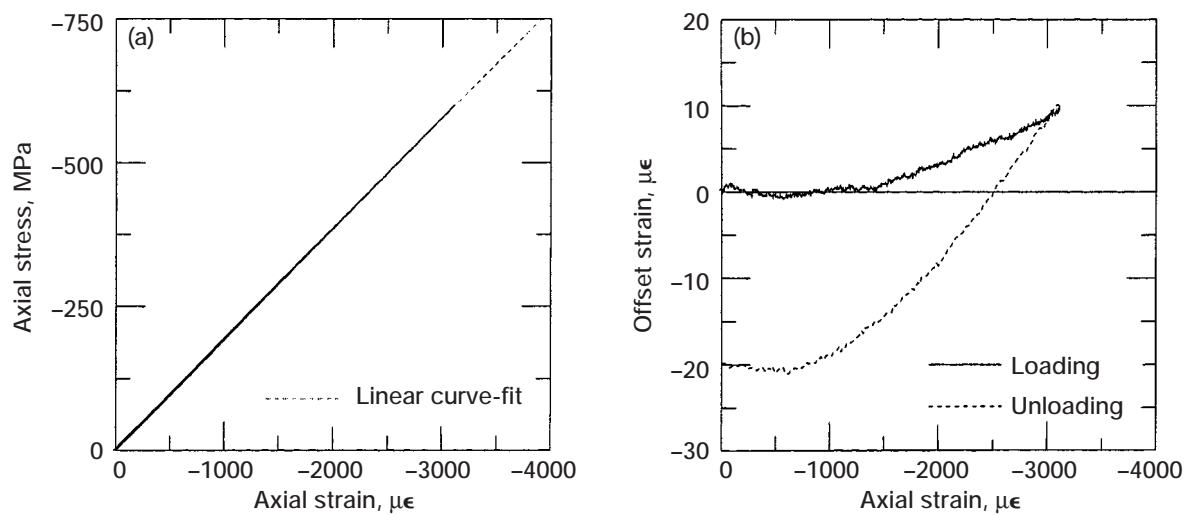


Figure 7.—SiC/Ti-15-3 thick plate response to compressive loading portion of loading sequence 1 at 23 °C. (a) Stress-strain with linear loading line shown. (b) Offset strain-total strain indicating stiffening.

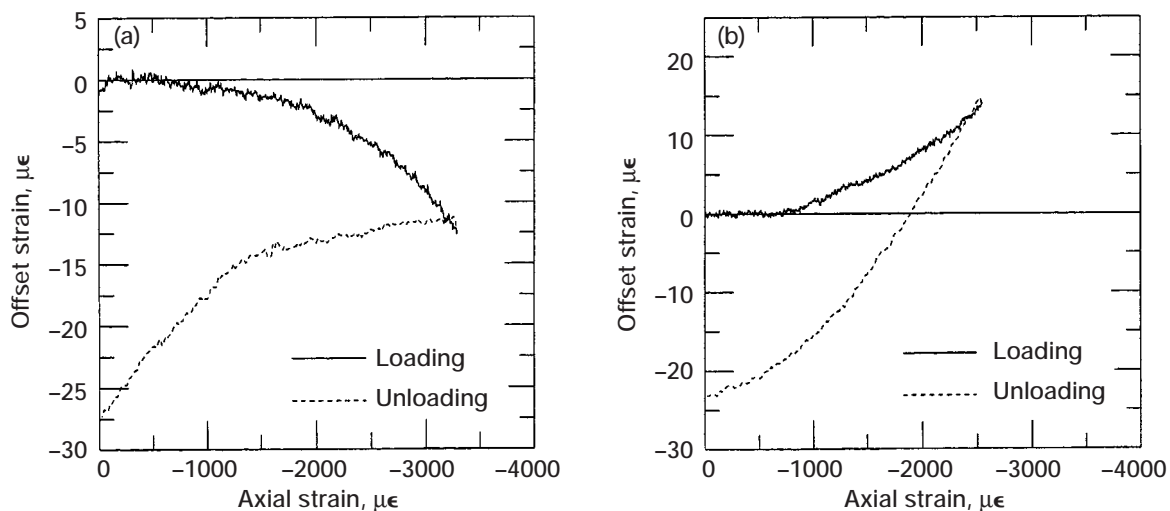


Figure 8.—SiC/Ti-15-3 thick plate response to compressive loading portion of loading sequence 2 at 23 °C. (a) Showing no stiffening. (b) Indicating stiffening.

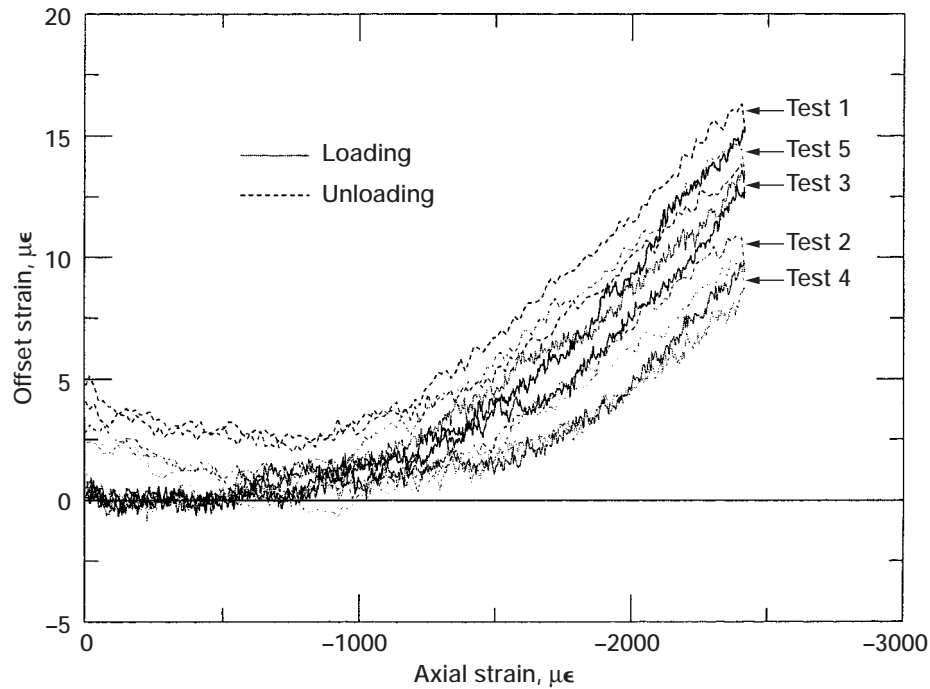


Figure 9.—SiC/Ti-15-3 thick plate response to loading sequence 3 at 23 °C indicating stiffening to different levels for maximum stress of -500 MPa.

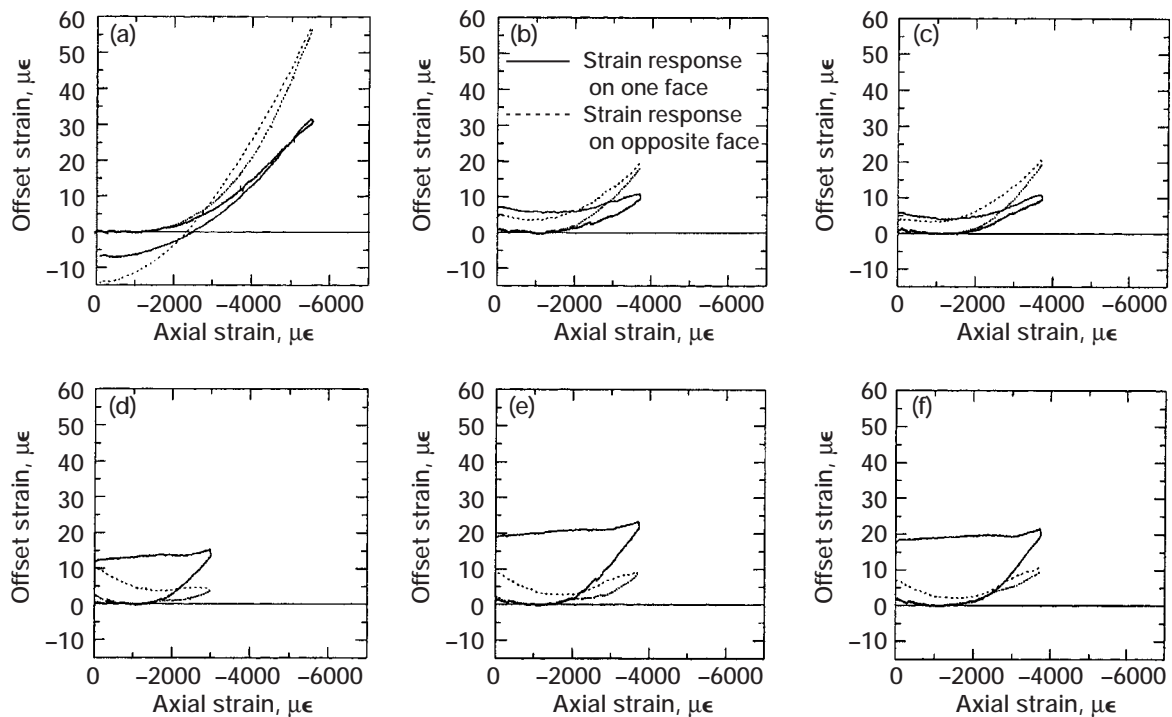


Figure 10.—SiC/Ti-15-3 thick plate response to loading sequence 1 at 23 °C as measured by strain gages mounted on opposite sides of specimen. (a) First experimental setup; loaded to a compressive stress of 1034 MPa. (b) First experimental setup; loaded to a compressive stress of 690 MPa. (c) First experimental setup; loaded to a compressive stress of 690 MPa. (d) Second experimental setup; loaded to a compressive stress of 552 MPa. (e) Second experimental setup; loaded to a compressive stress of 690 MPa. (f) Second experimental setup; loaded to a compressive stress of 690 MPa.

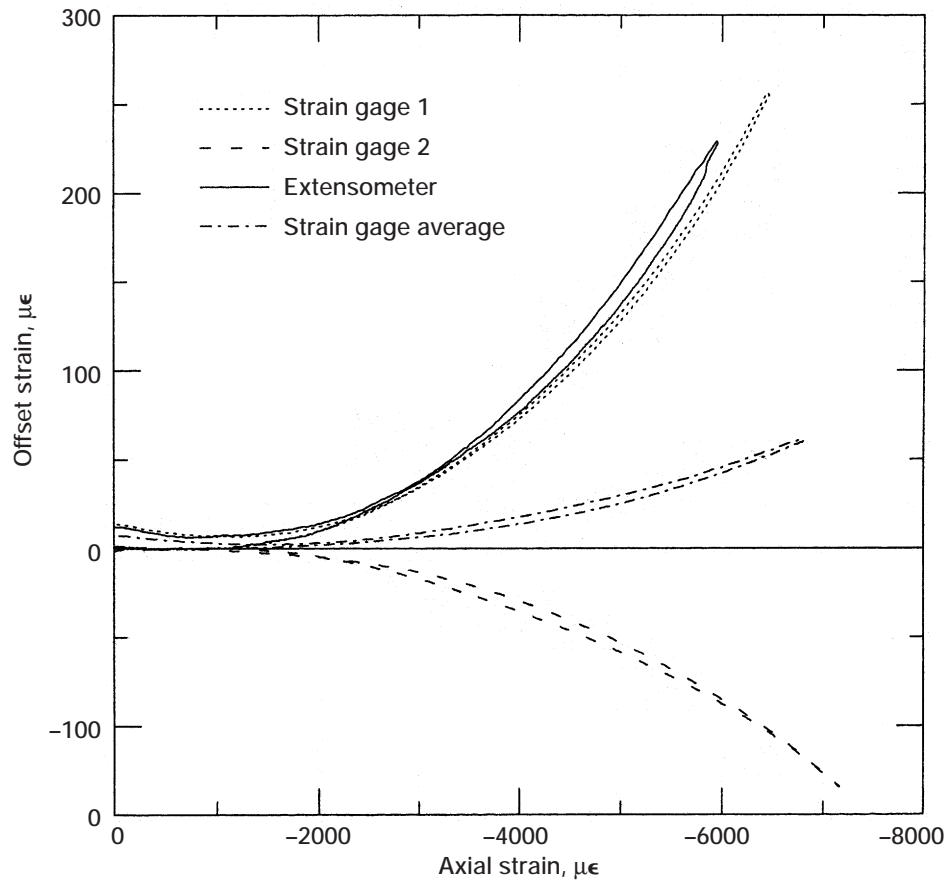


Figure 11.—SiC/Ti-15-3 thick plate compression response at 23 °C. Strain gage 1 and extensometer were mounted on same side of specimen and strain gage 2 was on opposite side.

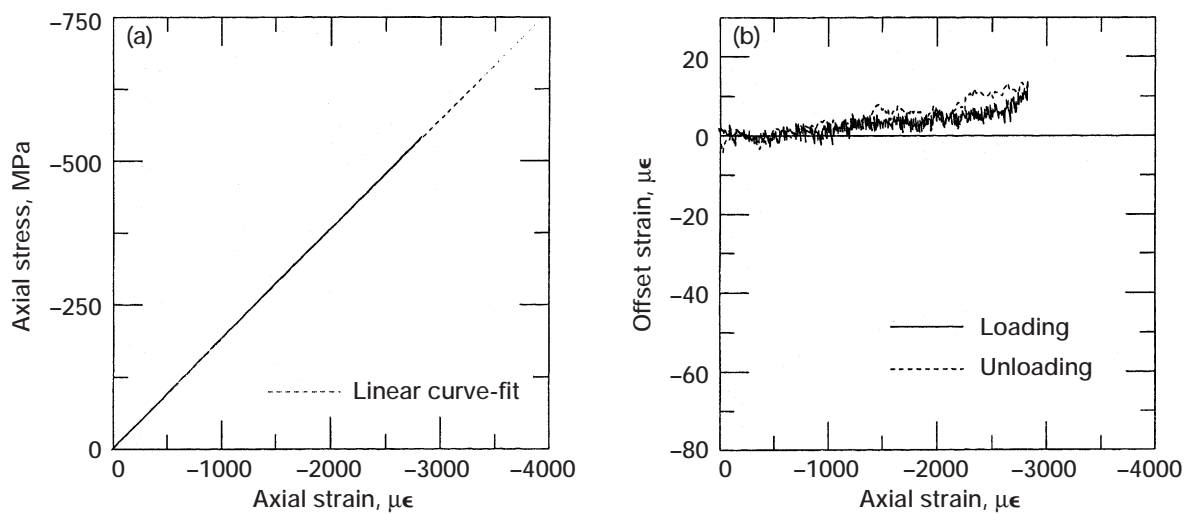


Figure 12.—SiC/Ti-15-3 thick plate compression response to loading sequence 1 at 427 °C. (a) Stress-strain with linear loading line shown. (b) Offset strain-total strain indicating stiffening.

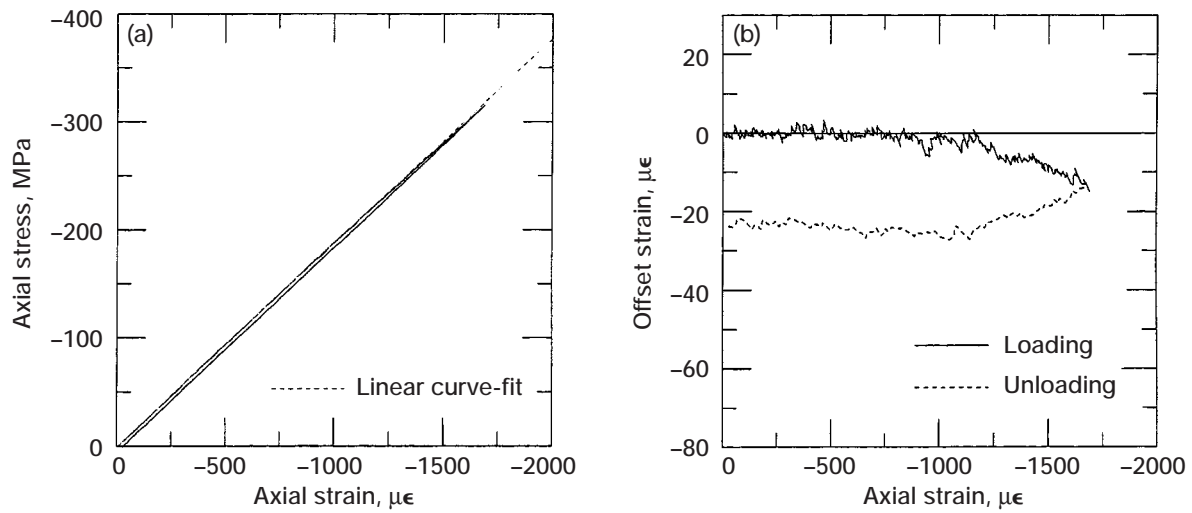


Figure 13.—SiC/Ti-15-3 thick plate compression response to loading sequence 1 at 482 °C. (a) Stress-strain with linear loading line shown. (b) Offset strain-total strain indicating no stiffening.

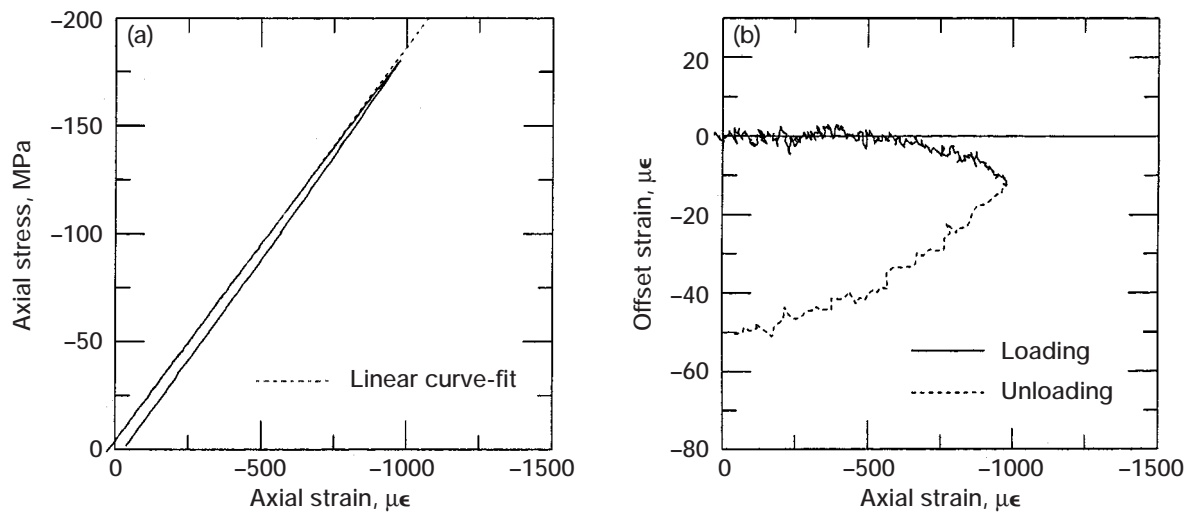


Figure 14.—SiC/Ti-15-3 thick plate compression response to loading sequence 1 at 538 °C. (a) Stress-strain with linear loading line shown. (b) Offset strain-total strain indicating no stiffening.

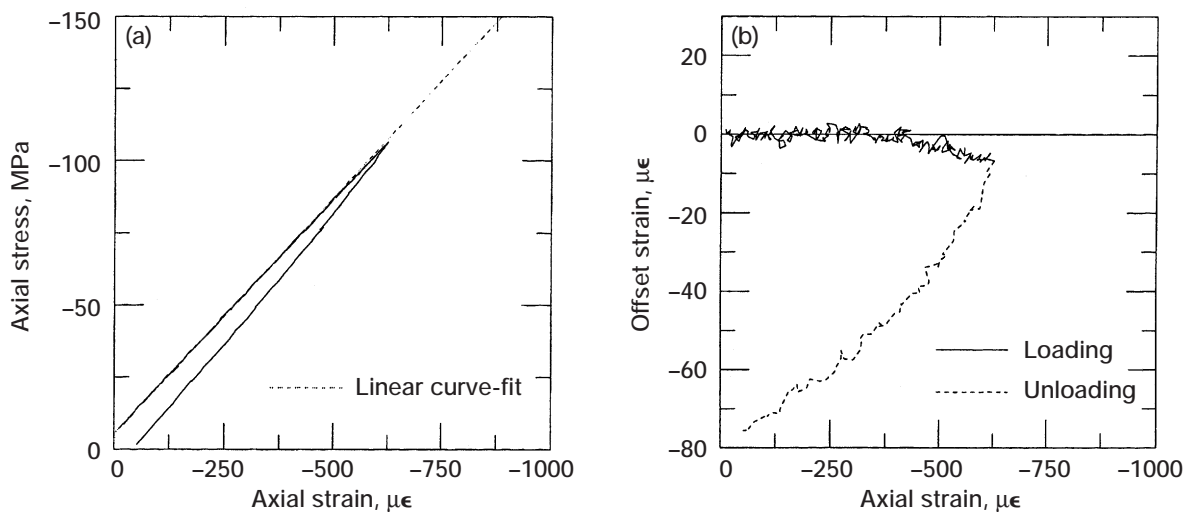


Figure 15.—SiC/Ti-15-3 thick plate compression response to loading sequence 1 at 649 °C. (a) Stress-strain with linear loading line shown. (b) Offset strain-total strain indicating no stiffening.

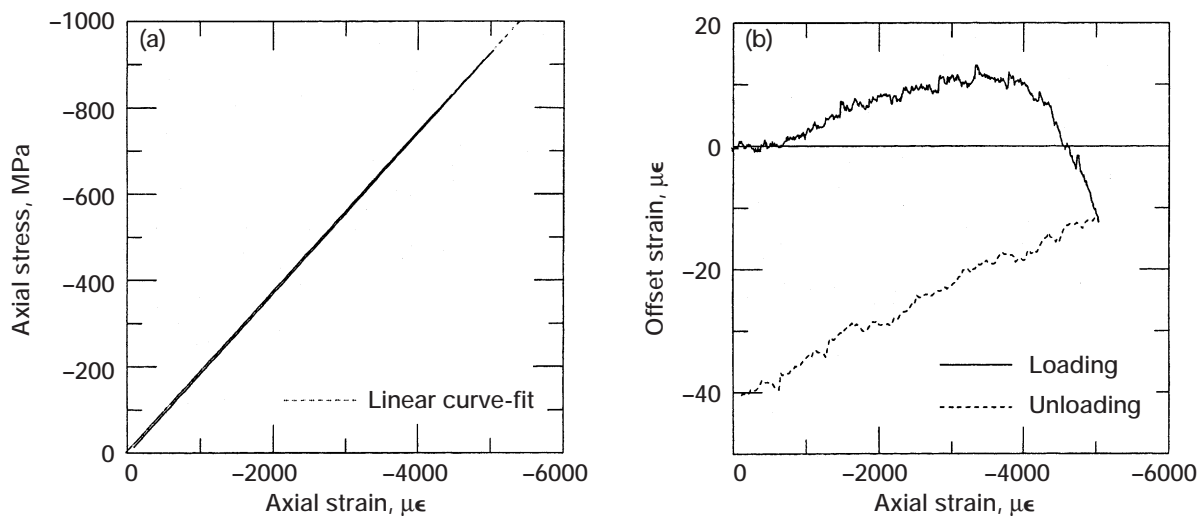


Figure 16.—SiC/Ti-15-3 thick plate compression response to loading sequence 1 at 427 °C; unloading occurred when offset strain reached $-10 \mu\epsilon$. (a) Stress-strain with linear loading line shown. (b) Offset strain-total strain indicating stiffening.

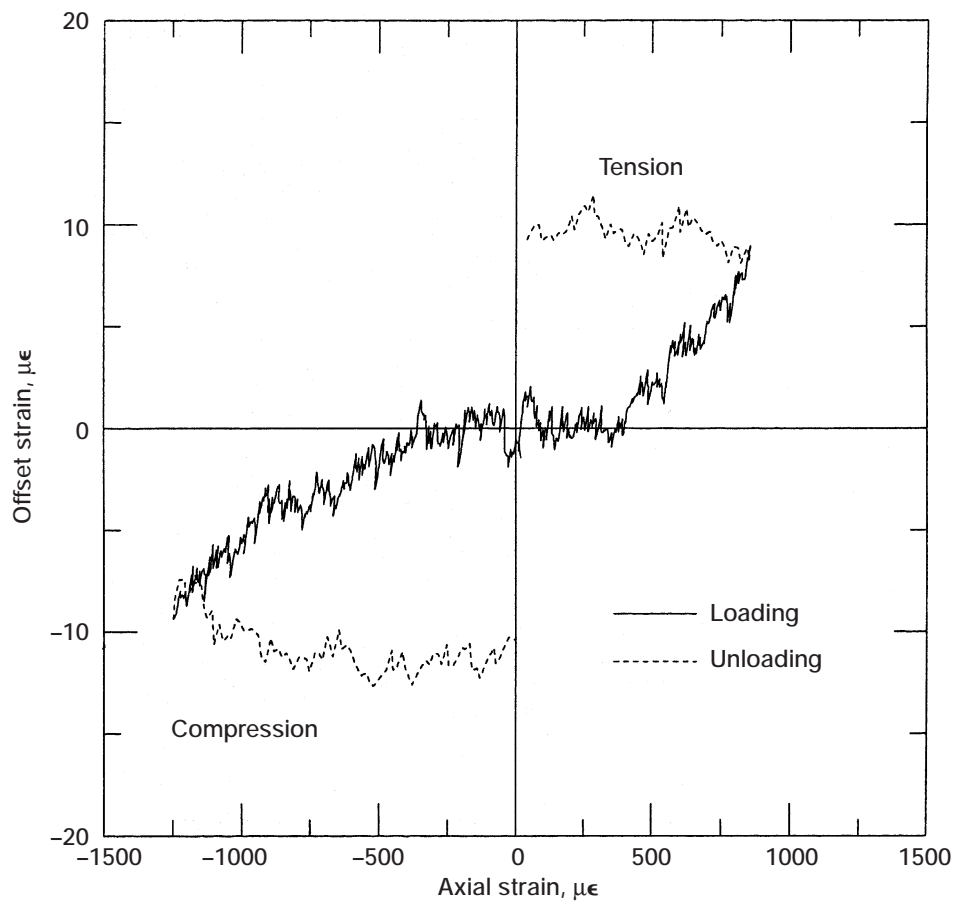


Figure 17.—SiC/Ti-15-3 thick plate response to loading sequence 1 at 482 °C.

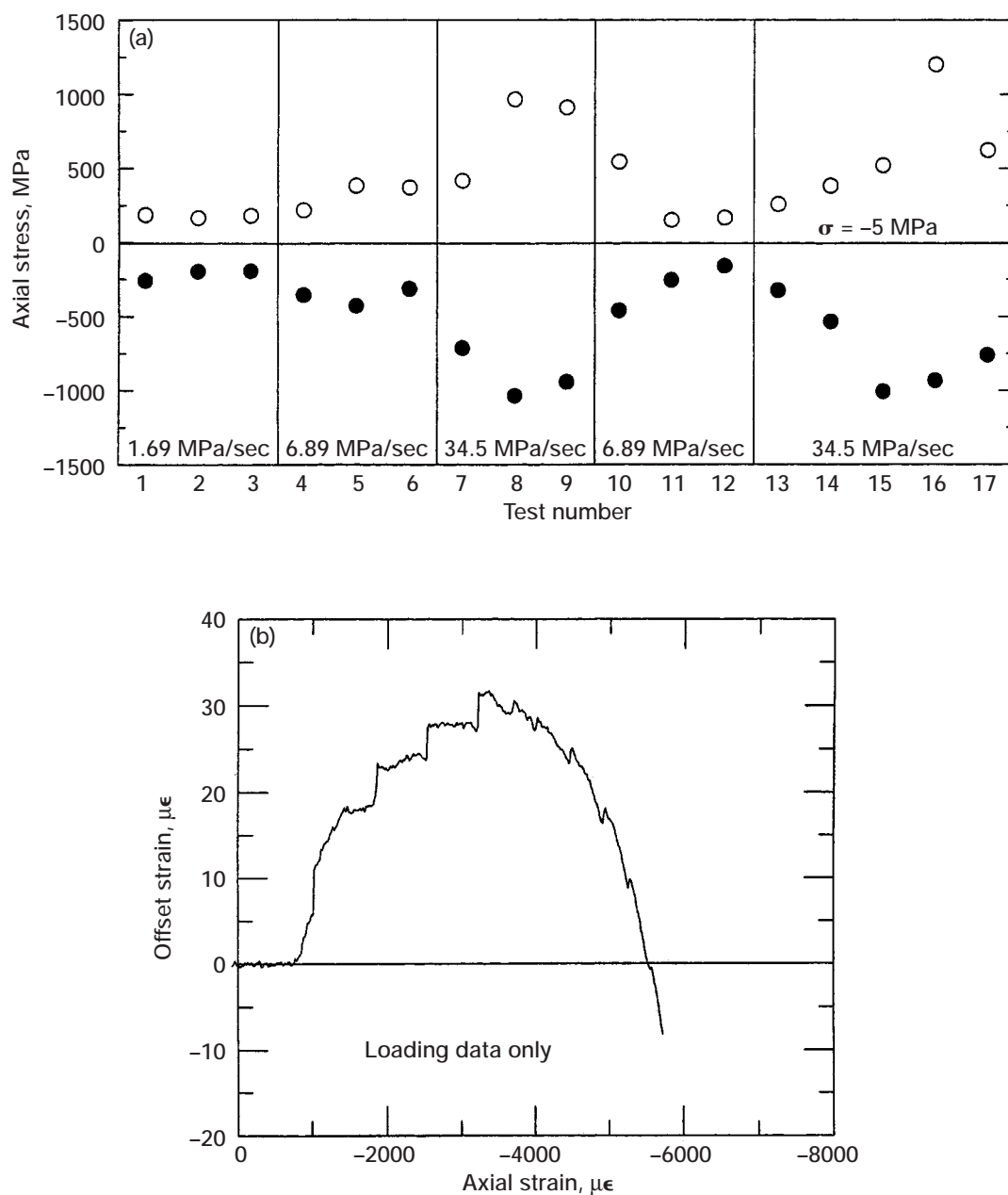


Figure 18.—SiC/Ti-15-3 thick plate response to loading sequence 1 at 482 °C. (a) Stress at load reversal versus loading rate. (b) Compressive strain response for loading rate of 34.5 MPa/sec.

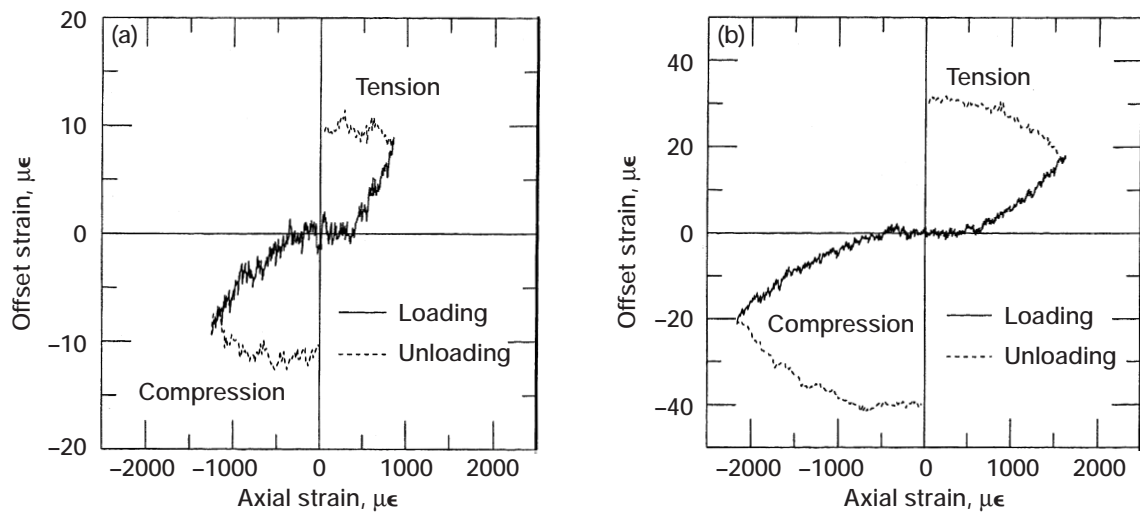


Figure 19.—SiC/Ti-15-3 thick plate response to loading sequence 1 at 482 °C and loading rate of 6.89 MPa/sec. (a) 10 $\mu\epsilon$ offset target value. (b) 20 $\mu\epsilon$ offset target value.

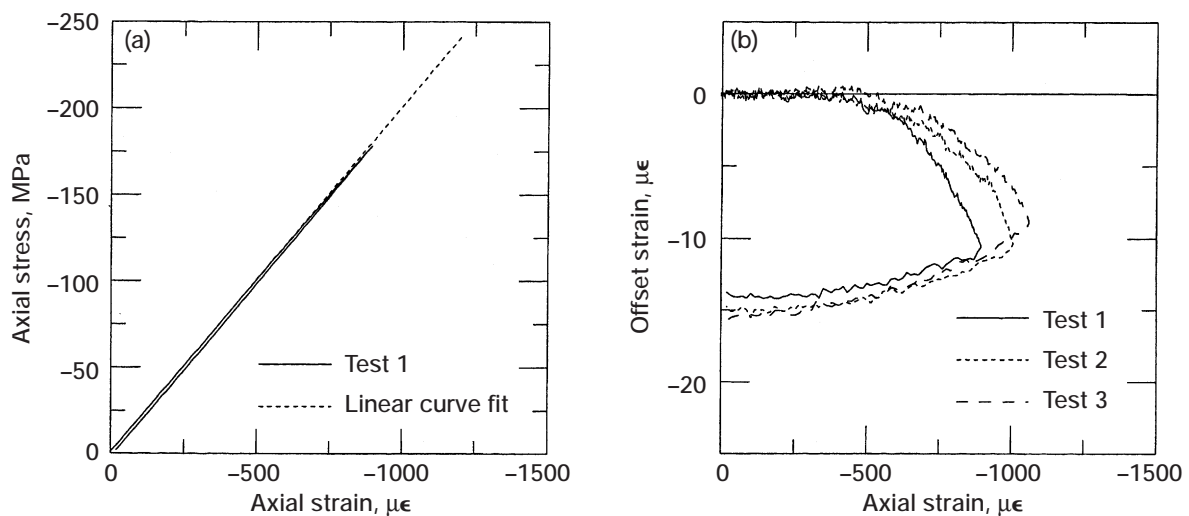


Figure 20.—Solution annealed IN-718 response to compressive loading at 23 °C. (a) Stress-strain with linear loading line shown. (b) Offset strain-total strain indicating no stiffening.

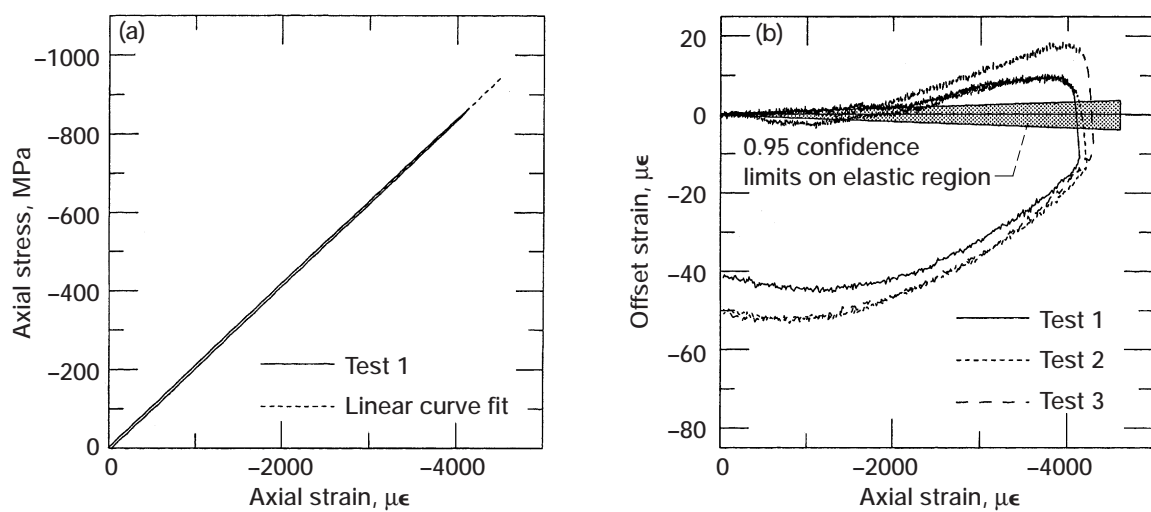


Figure 21.—Thermally aged IN-718 response to compressive loading at 23 °C. (a) Stress-strain with linear loading line shown. (b) Offset strain-total strain indicating initial stiffening.

REPORT DOCUMENTATION PAGE			Form Approved OMB No. 0704-0188	
Public reporting burden for this collection of information is estimated to average 1 hour per response, including the time for reviewing instructions, searching existing data sources, gathering and maintaining the data needed, and completing and reviewing the collection of information. Send comments regarding this burden estimate or any other aspect of this collection of information, including suggestions for reducing this burden, to Washington Headquarters Services, Directorate for Information Operations and Reports, 1215 Jefferson Davis Highway, Suite 1204, Arlington, VA 22202-4302, and to the Office of Management and Budget, Paperwork Reduction Project (0704-0188), Washington, DC 20503.				
1. AGENCY USE ONLY (Leave blank)		2. REPORT DATE July 1998		3. REPORT TYPE AND DATES COVERED Technical Memorandum
4. TITLE AND SUBTITLE Investigation of Anomalous Behavior in Metallic-Based Materials Under Compressive Loading			5. FUNDING NUMBERS WU-523-21-13-00	
6. AUTHOR(S) Christopher M. Gil, Cliff J. Lissenden, and Bradley A. Lerch				
7. PERFORMING ORGANIZATION NAME(S) AND ADDRESS(ES) National Aeronautics and Space Administration Lewis Research Center Cleveland, Ohio 44135-3191			8. PERFORMING ORGANIZATION REPORT NUMBER E-11107	
9. SPONSORING/MONITORING AGENCY NAME(S) AND ADDRESS(ES) National Aeronautics and Space Administration Washington, DC 20546-0001			10. SPONSORING/MONITORING AGENCY REPORT NUMBER NASA TM-1998-206640	
11. SUPPLEMENTARY NOTES Christopher M. Gil, and Cliff J. Lissenden, Pennsylvania State University, University Park, Pennsylvania; Bradley A. Lerch, NASA Lewis Research Center. Responsible person, Bradley A. Lerch, organization code 5920, (216) 433-5522.				
12a. DISTRIBUTION/AVAILABILITY STATEMENT Unclassified - Unlimited Subject Category: 24 This publication is available from the NASA Center for AeroSpace Information, (301) 621-0390.			12b. DISTRIBUTION CODE	
13. ABSTRACT (Maximum 200 words) An anomalous material response has been observed under the action of applied compressive loads in fibrous SiC/Ti (both Ti-6242 and Ti-15-3 alloys) and the monolithic nickel-base alloy IN-718 in the aged condition. The observed behavior is an increase, rather than a decrease, in the instantaneous Young's modulus with increasing load. This increase is small, but can be significant in yield surface determination tests, where an equivalent offset strain on the order of 10 µε (10×10 ⁻⁶ m/m) is being used. Stiffening has been quantified by calculating offset strains from the linear elastic loading line. The offset strains associated with stiffening during compressive loading are positive and of the same order as the target offset strains in yield surface determination tests. At this time we do not have a reasonable explanation for this response nor can we identify a deformation mechanism that might cause it. On the other hand, we are not convinced that it is an artifact of the experimental procedure because a number of issues have been identified and seemingly ruled out. In fact, stiffening appears to be temperature dependent, since it decreases as the temperature increases.				
14. SUBJECT TERMS Composite; Plasticity; Yield surface; Stiffening; SiC/Ti; Nickel alloy			15. NUMBER OF PAGES 29	
			16. PRICE CODE A03	
17. SECURITY CLASSIFICATION OF REPORT Unclassified	18. SECURITY CLASSIFICATION OF THIS PAGE Unclassified	19. SECURITY CLASSIFICATION OF ABSTRACT Unclassified	20. LIMITATION OF ABSTRACT	